Supplementary Information

Structure-guided combination therapy to potently improve the function of mutant CFTRs

Guido Veit*, Haijin Xu, Elise Dreano, Radu G Avramescu, Miklos Bagdany, Lenore K Beitel, Ariel Roldan, Mark A Hancock, Cecilia Lay, Wei Li, Katelin Morin, Sandra Gao, Puiying A Mak, Edward Ainscow, Anthony P Orth, Peter McNamara, Aleksander Edelman, Saul Frenkiel, Elias Matouk, Isabelle Sermet-Gaudelus, William G Barnes, Gergely L Lukacs*

*Corresponding authors:

G. L. Lukacs: Department of Physiology, McGill University
3655 Promenade Sir-William-Osler, Montreal, Quebec H3G 1Y6, Canada.
E-mail: gergely.lukacs@mcgill.ca, Ph: (514) 398-5582

G. Veit: Department of Physiology, McGill University
3655 Promenade Sir-William-Osler, Montreal, Quebec H3G 1Y6, Canada.
E-mail: guido.veit@mcgill.ca, Ph: (514) 398-6190

This file contains:

Supplementary Figures 1-11
Supplementary Tables 1-3

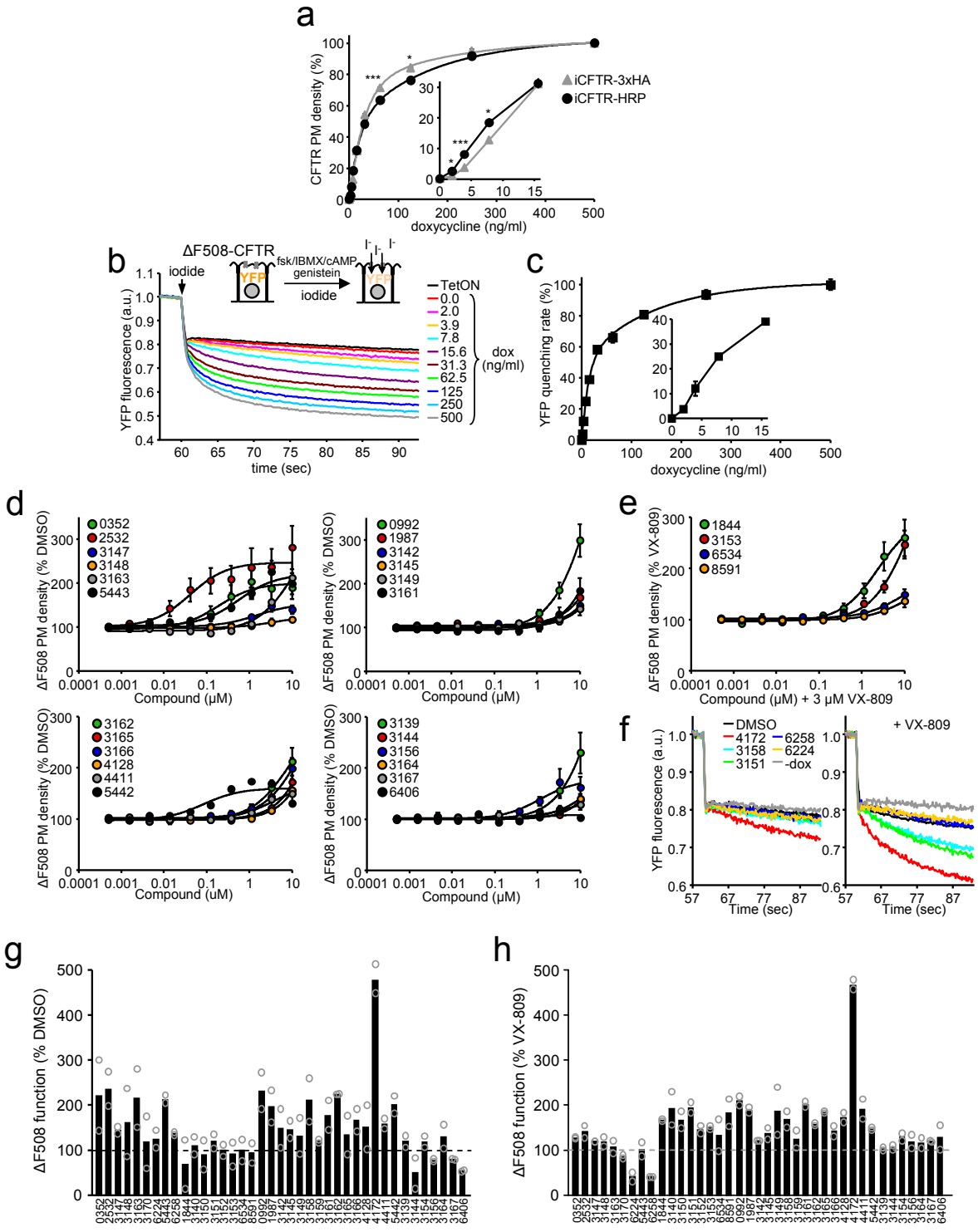

Supplementary Figure 1. Comparison between HTS assays and corrector concentration-dependent effect on the PM density and function in ΔF508-CFTR CFBE41o-. (**a**) PM density of 3xHA- or HRP-tagged WT-CFTR expression induced by increasing doxycyline concentrations (0-500 ng/ml) is expressed as percent of maximal signal. The HRP-tag increases the dynamic range of CFTR detection sensitivity (*n* = 3). (**b**) Schematic depiction of the halide-sensitive YFP quenching assay (upper part) and representative traces of WT-CFTR function. WT-CFTR expression was induced with increasing doxycyline concentrations (0-500 ng/ml). TetON CFBE41o- cells without CFTR expression served as control. (**c**) Quantification of the doxycyline induced WT-CFTR activity (*n* = 3). (**d,e**) The effect of treatment with the indicated correctors (24 hours, 37°C) alone (**d**) or in presence of VX-809 (3 μM, **e**) on the ΔF508-CFTR PM expression in CFBE41o- was determined by PM ELISA and is expressed as dose-response in percent of untreated controls (*n* = 3-57). (**f-h**) Effect of corrector treatment (10 μM, 24 hours, 37°C) alone (**g**) or in presence of VX-809 (**h**) on the ΔF508-CFTR function, determined by halide-sensitive YFP quenching assay (*n* = 2). Representative traces are shown in **f**. Data in **a**, **c-e** and **g-h** are means ± SEM of the indicated number of independent experiments. **P* < 0.05, ****P* < 0.001 by unpaired two-tailed Student's t-test. The precise P-values are listed in **Supplementary Table 4**.

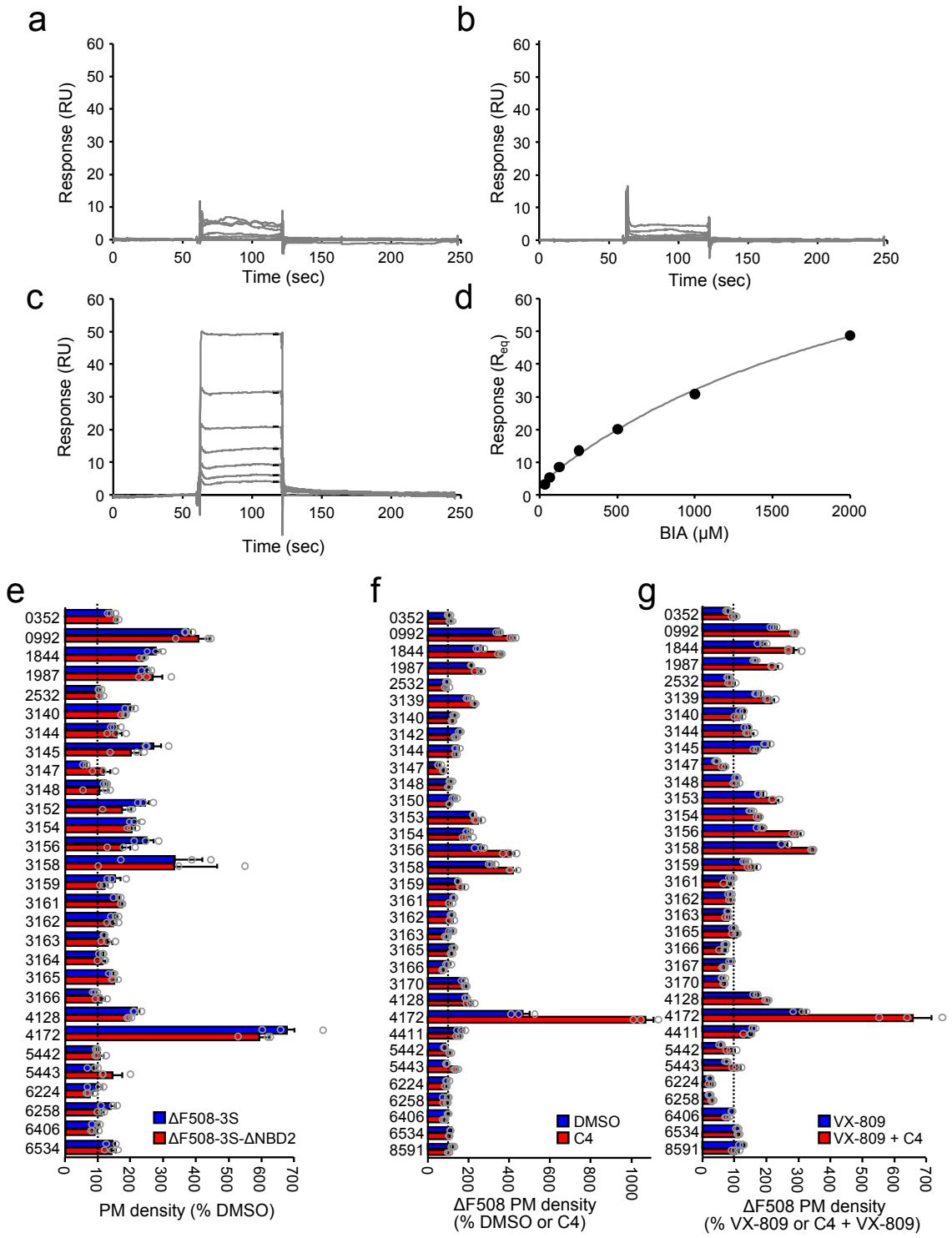

Supplementary Figure 2. Corrector mechanism of action. (**a-d**) Representative surface plasmon resonance (SPR) sensograms of 3151 (0-200 μM, **a**), 6258 (0-60 μM, **b**) or BIA (0-2000 μM, **c**) interaction with immobilized ΔF508-NBD1-1S. The binding isotherm for BIA is shown in **d**. (**e**) The effect of indicated correctors (10 μM, 24 hours) on the PM density of ΔF508-CFTR-3S (containing the solubilizing mutations F494N, Q637R, F492S) or ΔF508-CFTR-3S lacking the NBD2 domain (ΔNBD2) expressed as percent of untreated CFBE41o- cells (*n* = 3). (**f**,**g**) The effect of C4 (10 μM, 24 hours) on the PM density of ΔF508-CFTR in CFBE41o- treated with the indicated correctors (10 μM) alone (**f**, *n* = 3) or in combination with 3 μM VX-809 (**g**, *n* = 3). Data in **e-g** are means ± SEM of the indicated number of independent experiments.

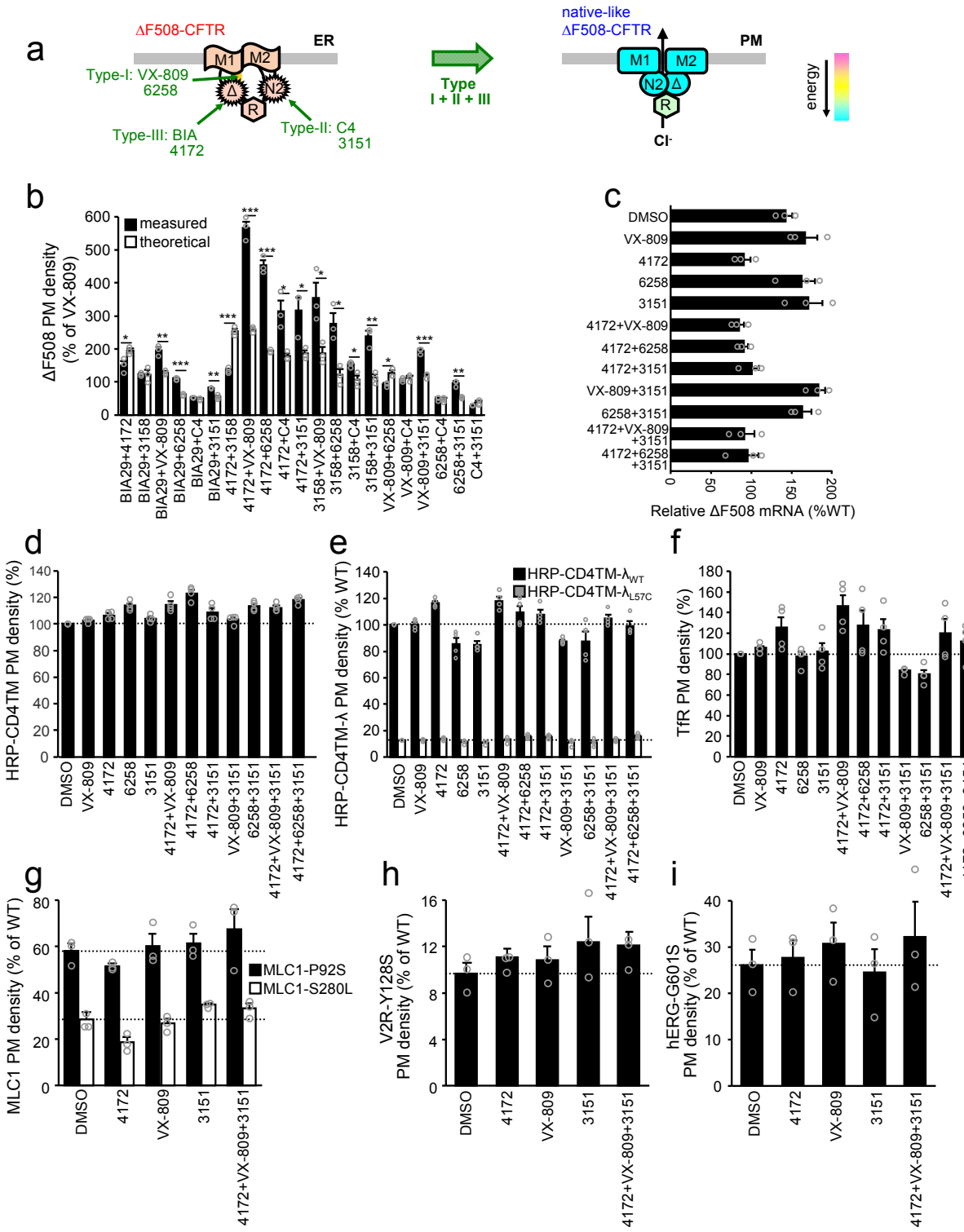

Supplementary Figure 3. Corrector combinations rescue the PM density of ΔF508-CFTR but do not affect other native or conformationally defective membrane proteins. (**a**) Schematic depiction of the domain structure of CFTR and the misfolding associated with the ΔF508 mutation[17]. Combination of different compound types that target distinct folding defects can restore the conformational stability of ΔF508-CFTR near to the WT-level. (**b**) Effect of indicated correctors combinations (4172, 3151, C4 - 10 μM; VX-809, 6258 - 3 μM, BIA29 - 250 μM, 24 hours, 37°C) on the PM density of ΔF508-CFTR in comparison to the calculated additivity of single corrector effects in CFBE41o- (n = 3). *P < 0.05, **P < 0.01, ***P < 0.001 by unpaired two-tailed Student's t-test. The precise P-values are listed in **Supplementary Table 4**. (**c**) WT- and ΔF508-CFTR mRNA expression in CFBE41o- with and without corrector treatment determined by qPCR (n = 3). (**d-i**) Effect of the indicated single correctors and corrector combinations on the PM density of HRP-CD4TM (**d**, n = 4), HRP-CD4TM-λ_{WT} and -λ_{L57C} (**e**, n = 4), TfR (**f**, n = 4), MLC1-P92S and -S280L (**g**, n = 3), V2R-Y128S (**h**, n = 3) and hERG-G601S (**i**, n = 3). Data in **b-i** are means ± SEM of the indicated number of independent experiments.

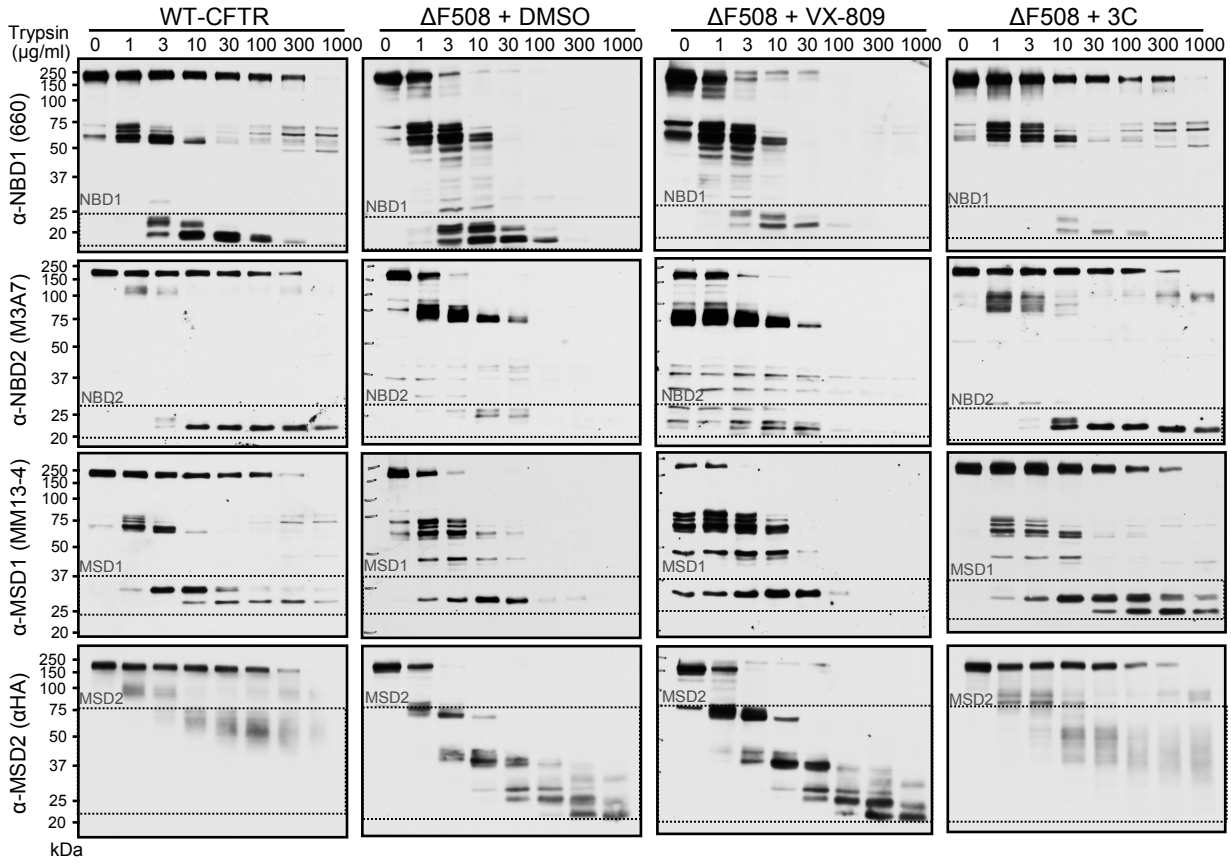

Supplementary Figure 4. *In situ* protease susceptibility of WT and ΔF508-CFTR. The WT- or ΔF508-CFTR conformation was probed by limited trypsinolysis and immunoblotting in isolated microsomes. Microsomes isolated from BHK-21 cells, treated with DMSO, VX-809 or 3C combination, were exposed to increasing concentrations of trypsin for 15 minutes on ice and the remaining full-length CFTR as well as CFTR fragments were visualized by immunoblotting with the domain specific antibodies 660, M3A7, MM13-4 and αHA to detect NBD1, NBD2, MSD1, and MSD2 containing fragments, respectively. The molecular weights of domains and their fragments are indicated with labeled dotted boxes. Representative immunoblots of *n* = 4 independent experiments.

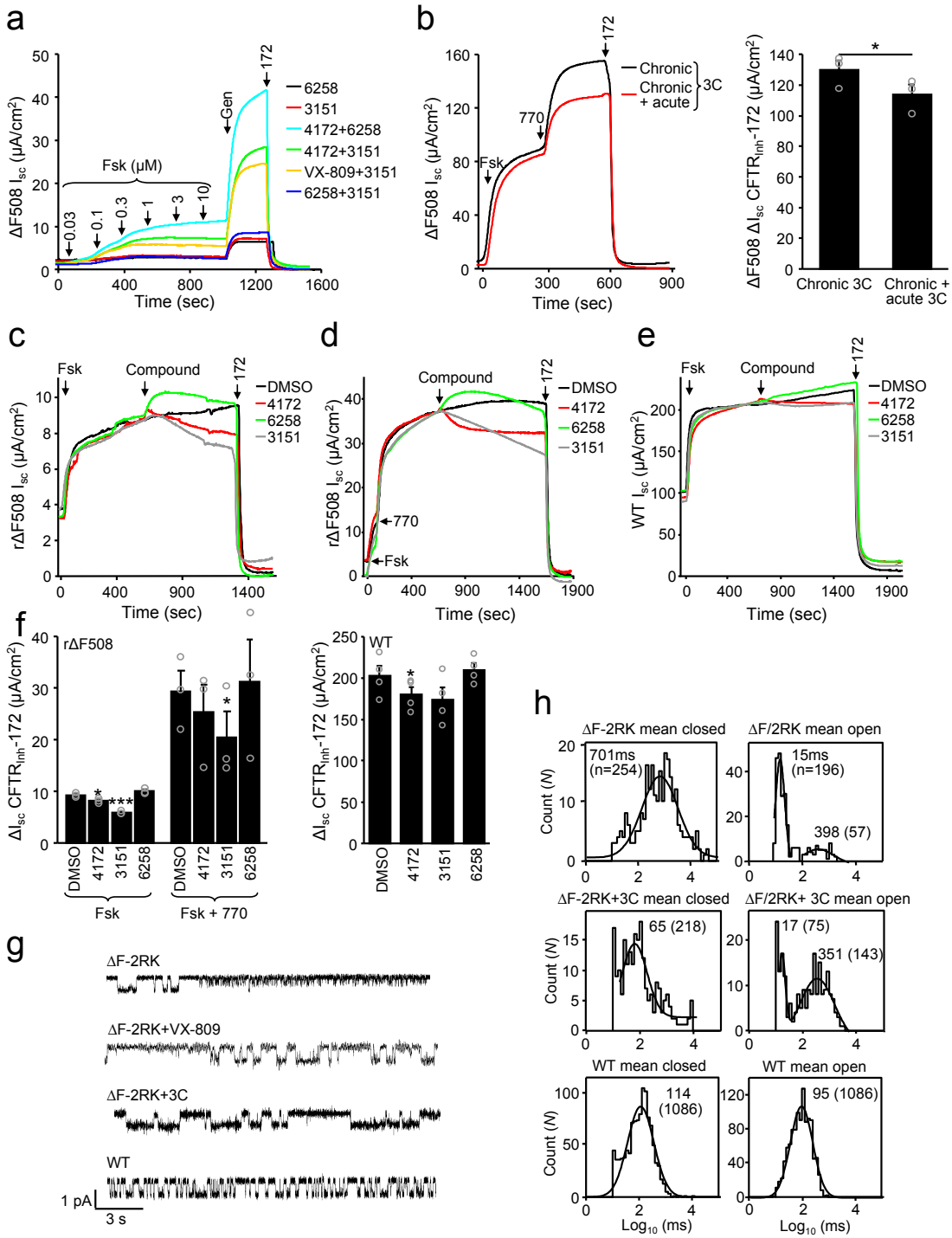

Supplementary Figure 5. Corrector effect on the function of ΔF508-CFTR. (**a**) Representative traces for the effect of indicated single correctors or corrector combinations on the Isc of ΔF508-CFTR in CFBE41o-. CFTR-mediated short-circuit currents (I_{sc}) were induced by sequential acute addition of increasing concentrations of forskolin (Fsk) and genistein (Gen, 50 μM), followed by CFTR inhibition with $CFTR_{inh}$-172 (172, 20 μM) in the presence of a basolateral-to-apical chloride gradient after basolateral permeabilization with amphotericin B. The quantification of the CFTR-mediated currents is shown in **Figure 4d**. (**b**) Effect of 3C acute addition on the Isc of 3C corrected (chronic treatment: 24 hours, 37°C) ΔF508-CFTR. Left panel, representative traces; right panel, quantification of the $CFTR_{inh}$-172-sensitive Isc (n = 3). (**c-e**) Representative traces for acute effect of DMSO or correctors (4172, 3151 - 10 μM; 6258 - 3 μM) on the 20 μM forskolin activated I_{sc} of low-temperature rescued (**c**), and 10 μM VX-770 potentiated (**d**) ΔF508-CFTR (rΔF508) or forskolin activated WT-CFTR (**e**) in CFBE41o-. (**f**) Quantification of the acute effect of the indicated single corrector on the $CFTR_{inh}$-172-sensitive I_{sc} of rΔF508- (left panel, n = 3) and WT-CFTR (right panel, n = 4). (**g**) Representative traces of ΔF508-CFTR-2RK channel activity in presence or absence of VX-809 or 3C measured at 36˚C in BLM. For VX-809 and 3C parallel records over a temperature range ~27-36°C and with compressed time scale are shown in **Figure 4f**. WT-CFTR activity is shown as control. (**h**) Closed and open mean time histograms of single ΔF508-CFTR-2RK channels in presence of 3C. Histograms were fitted with one or two components Gaussian distribution. The mean closed and open times are indicated in ms, the number of events is specified in brackets. The histograms and values for untreated ΔF508-CFTR-2RK and WT-CFTR are shown for comparison[37]. Data in **b** and **f** are means ± SEM of the indicated number of independent experiments. *P < 0.05, ***P < 0.001 by unpaired two-tailed Student's t-test. The precise P-values are listed in **Supplementary Table 4**.

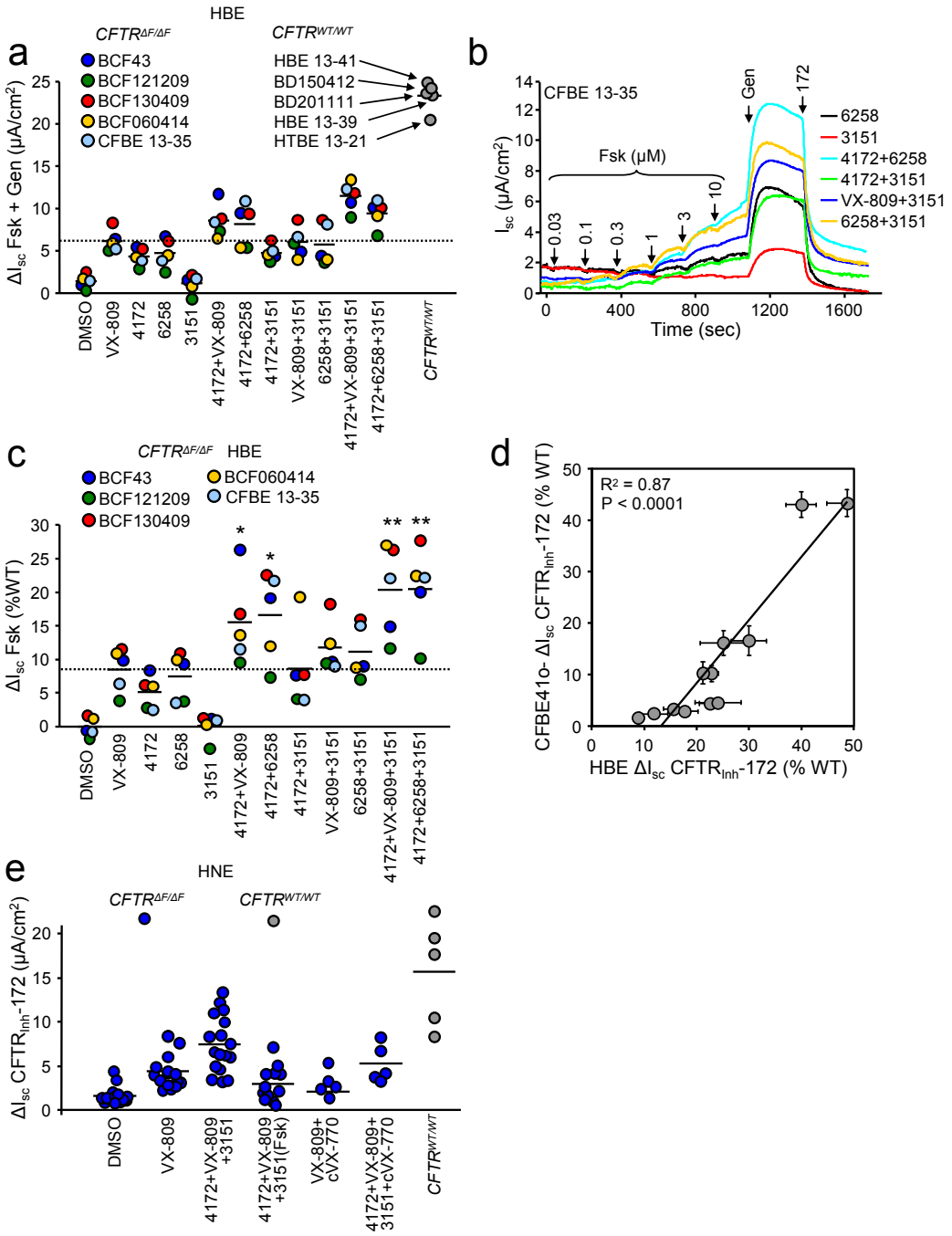

Supplementary Figure 6. Functional correction of ΔF508-CFTR in human bronchial and nasal epithelia. (**a,b**) Effect of indicated single correctors or corrector combinations on the I_{sc} of CF-HBE with *CFTR*$^{\Delta F508/\Delta F508}$ genotype. CFTR-mediated currents were induced by sequential acute addition of increasing concentrations of forskolin (Fsk) and genistein (Gen, 50 μM) followed by CFTR inhibition with $CFTR_{inh}$-172 (172, 20 μM) in an intact monolayer in the absence of trasepithelial chloride concentrations gradient. The Fsk- and Gen-stimulated current (ΔIsc Fsk + Gen) in HBE isolated from five donor lungs with *CFTR*$^{WT/WT}$ genotype or from five different homozygous ΔF508 individuals after single correctors or corrector combination treatment is expressed as current per cm^2 (**a**). The same results as percentage of WT-CFTR currents are depicted in **Figure 5b**. Representative traces are shown in **b**. (**c**) Quantification of the Fsk-stimulated current (ΔI_{sc} Fsk) in CF-HBE isolated from five different homozygous ΔF508 individuals after single correctors or corrector combination treatment expressed as percentage of the mean WT-CFTR currents from **a**. **P* < 0.05, ***P* < 0.01 by paired two-tailed Student's t-test in comparison to VX-809. The precise *P*-values are listed in **Supplementary Table 4**. (**d**) Correlation between the functional correction in CFBE41o- (*n* = 3 independent experiments) and CF-HBE (cells from *n* = 5 individuals). The Pearson correlation coefficient and the associated *P*-value are shown. (**e**) Effect of VX-809 or 3C on the I_{sc} of CF-HNE isolated from seventeen individuals with *CFTR*$^{\Delta F508/\Delta F508}$ genotype or from five WT-CFTR donors. CFTR-mediated currents were induced by sequential acute addition of increasing concentrations of forskolin and VX-770 (10 μM) followed by CFTR inhibition with $CFTRi_{nh}$-172 (20 μM) in an intact monolayer with basolateral-to-apical chloride gradient. The $CFTR_{inh}$-172 inhibited current is expressed per cm^2. The same results as percentage of WT-CFTR currents are depicted in **Figure 5d**. Horizontal lines indicate means in **a**, **c** and **e**.

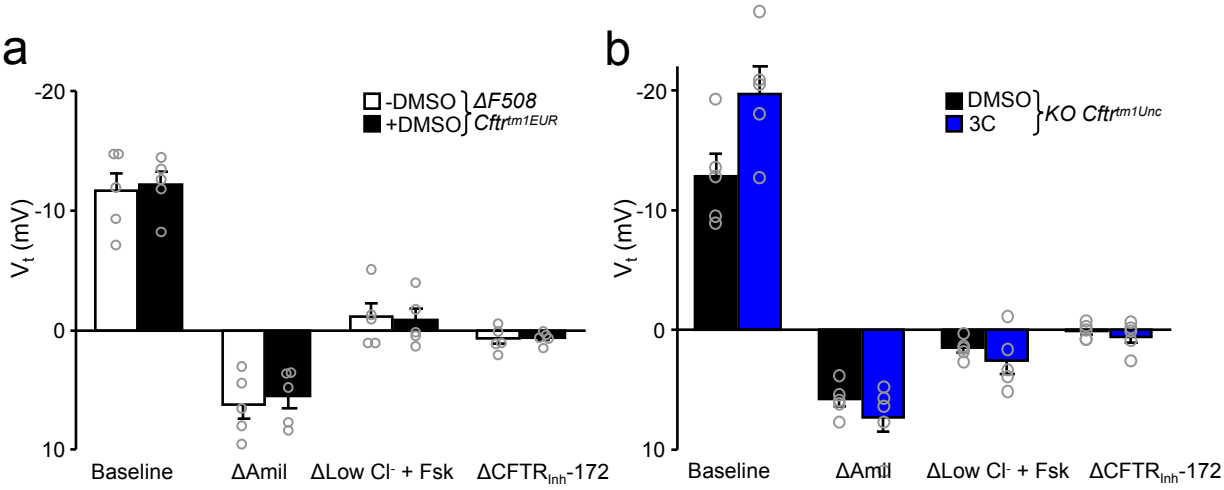

Supplementary Figure 7. 3C does not affect the NPD in *KO Cftr*^{tm1Unc} mice. (**a**) Effect of DMSO instillation on the baseline and V_t changes induced by the sequential addition of 100 µM amiloride (Amil), low Cl- + Fsk (10 µM) and 5 µM $CFTR_{inh}$-172 in *ΔF508 Cftr*^{tm1EUR} mice. Experiments were performed in 5 animals. Data are means ± SEM (**b**) Effect of 3C on the baseline and V_t changes induced by the sequential addition of amiloride, low Cl- + Fsk and $CFTR_{inh}$-172 in *KO Cftr*^{tm1Unc} mice. Experiments were performed in 5 animals. Data are means ± SEM.

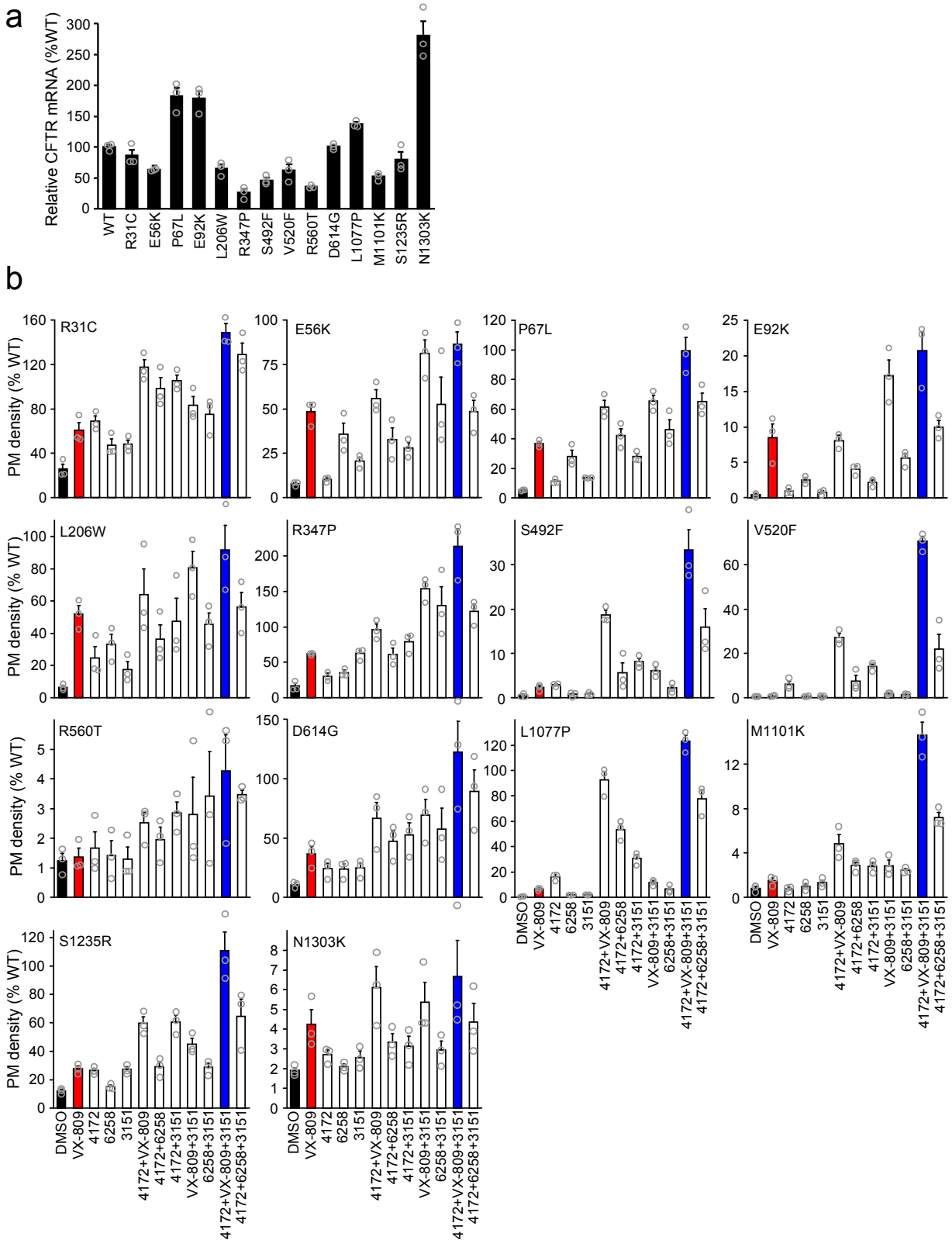

Supplementary Figure 8. Rescue of rare CF folding mutant PM density by allosteric corrector combination. (**a**) Mutant CFTR mRNA expression in CFBE41o- determined by qPCR and expressed as percent of WT-CFTR mRNA level (*n* = 3). (**b**) PM density of the indicated CFTR2 mutants alone and after indicated single correctors or corrector combinations treatment expressed as percentage of WT-CFTR in CFBE41o- (*n* = 3). The results for DMSO, VX-809 and 3C are shown as well in **Figure 6a**. Data are means ± SEM of the indicated number of independent experiments.

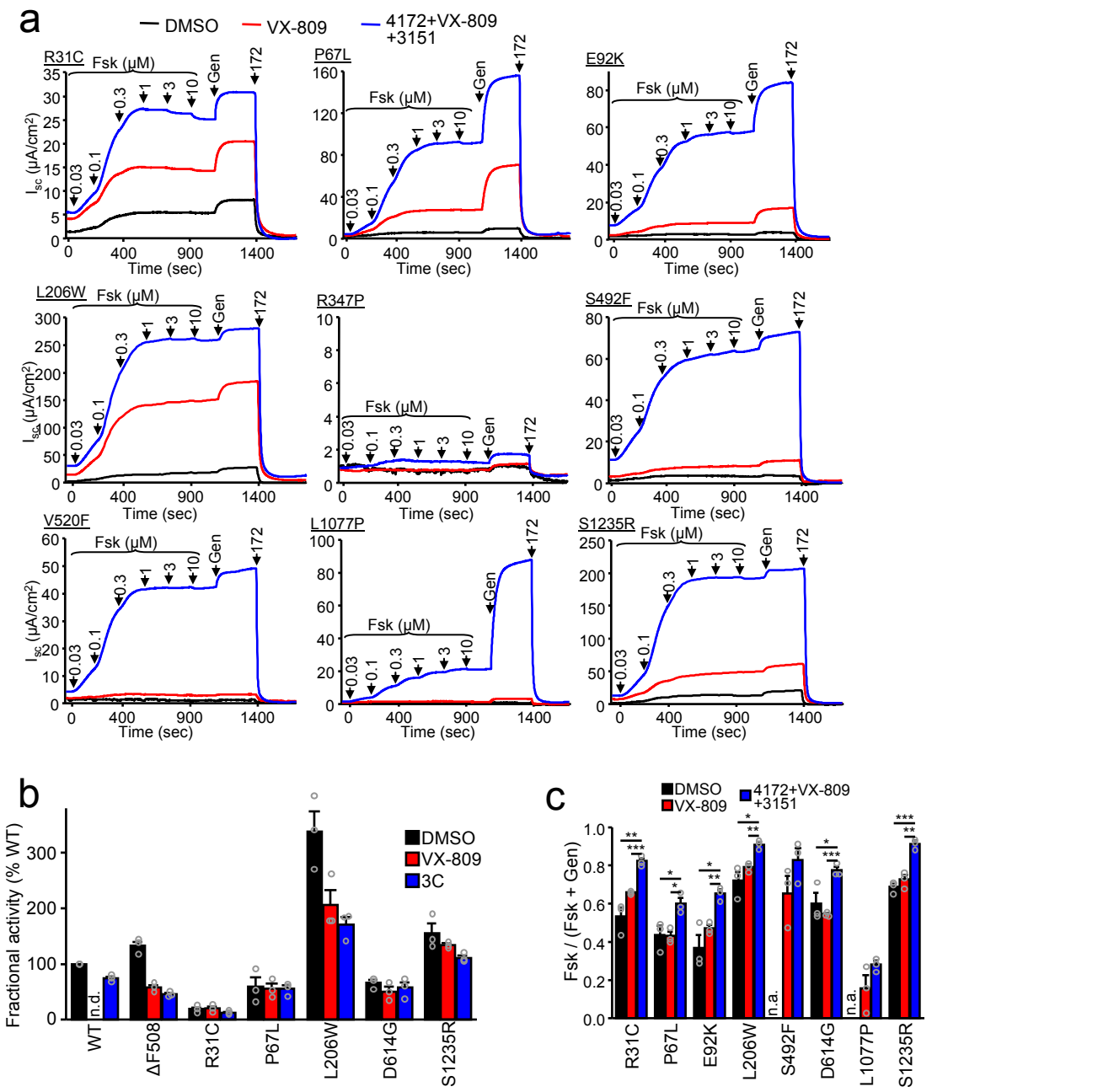

Supplementary Figure 9. Rescue of rare CF folding mutant function by allosteric corrector combination. (**a**) Representative traces for VX-809 or 3C effect on the I_{sc} of the indicated CFTR mutants in CFBE41o-. CFTR-mediated currents were induced by sequential acute addition of increasing forskolin (Fsk) concentrations and genistein (Gen, 50 μM) followed by CFTR inhibition with $CFTR_{inh}$-172 (172, 20 μM) in the presence of a basolateral-to-apical chloride gradient after basolateral permeabilization with amphotericin B. The quantification of the CFTR-mediated currents is shown in **Figure 6e**. (**b**) The fractional activity of mutant CFTR was calculated from the short-circuit current (I_{sc}) and PM density after correction with VX-809 or 3C and is shown as percentage of WT-CFTR expressing CFBE41o- (n = 3). (**c**) Fraction of potentiator independent current of the indicated CFTR mutants (n = 3). Data in **b** and **c** are means ± SEM of the indicated number of independent experiments. *P < 0.05, **P < 0.01, ***P < 0.001 by unpaired two-tailed Student's t-test. The precise P-values are listed in **Supplementary Table 4**.

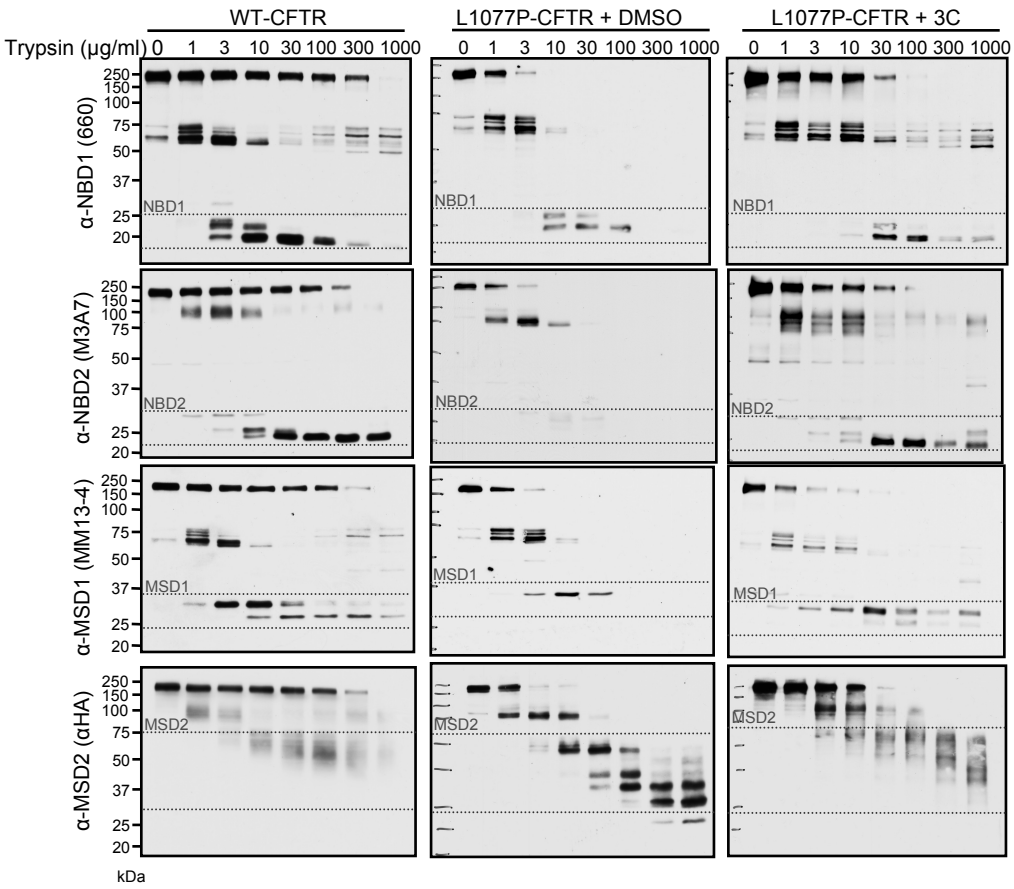

Supplementary Figure 10. In situ protease susceptibility of L1077P-CFTR with or without 3C correction in comparison to WT-CFTR. Microsomes were isolated from L1077P- or WT-CFTR-expressing BHK cells after 24 hours treatment with DMSO or 3C as indicated and subjected to limited trypsinolysis. Tryptic pattern of CFTRs were visualized by immunoblotting with the domain specific antibodies 660 to detect NBD1, M3A7 to detect NBD2, MM13-4 to detect MSD1 and αHA to detect MSD2 containing fragments. The molecular weights of the domain fragments are indicated by dotted lines. Representative immunoblots of $n = 4$ ($n = 3$ for the 660 antibody) independent experiments.

Fig. 2e

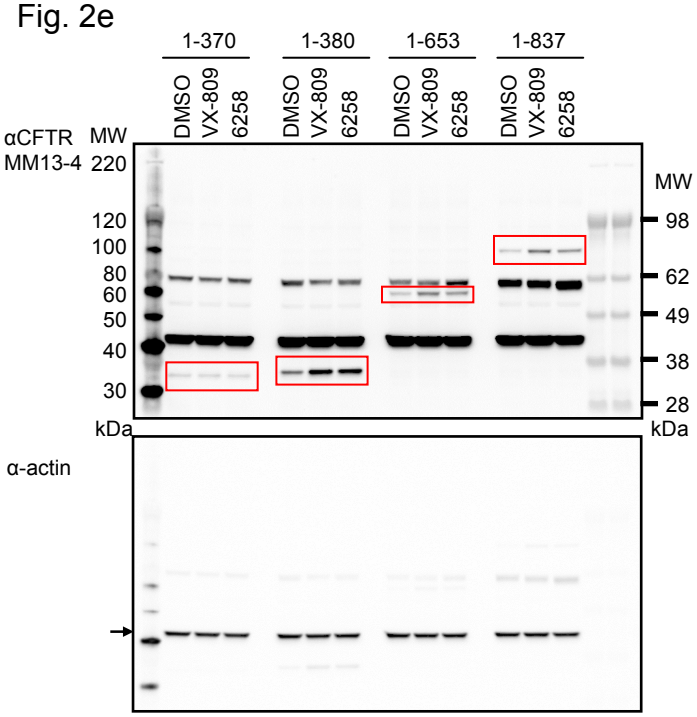

Fig. 3b

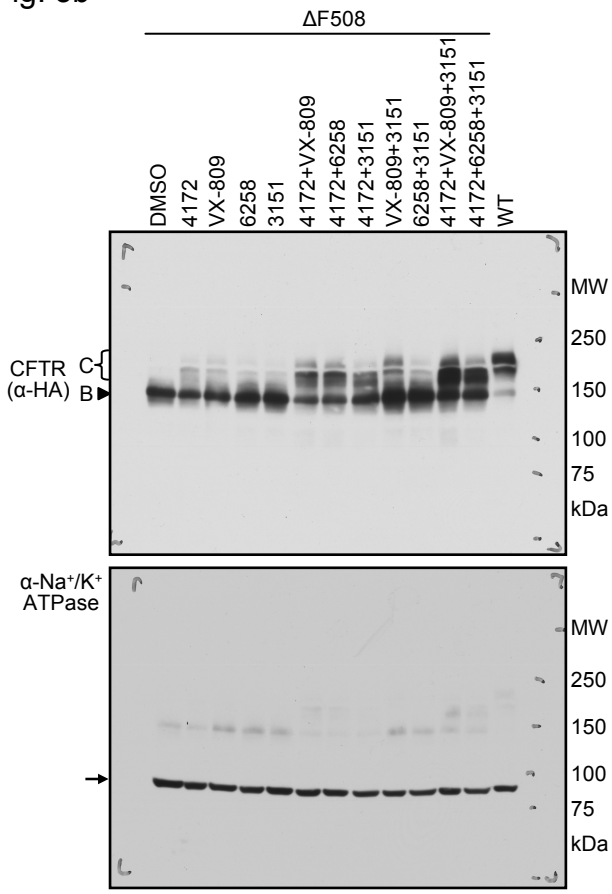

Fig. 3f

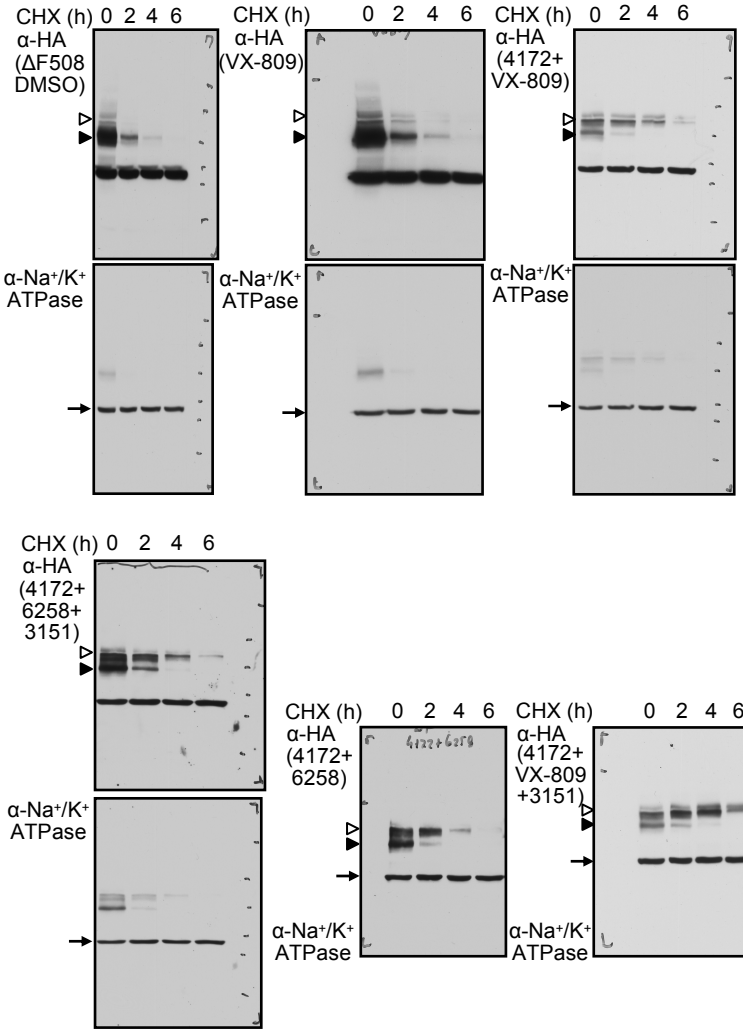

Fig. 3e

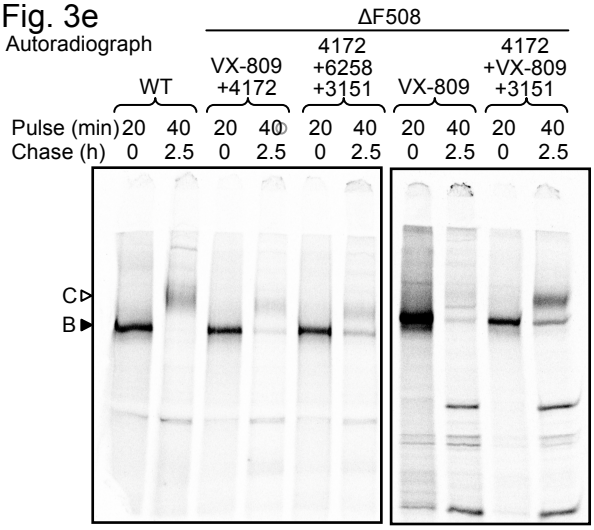

Supplementary Figure 11.

Fig. 4a

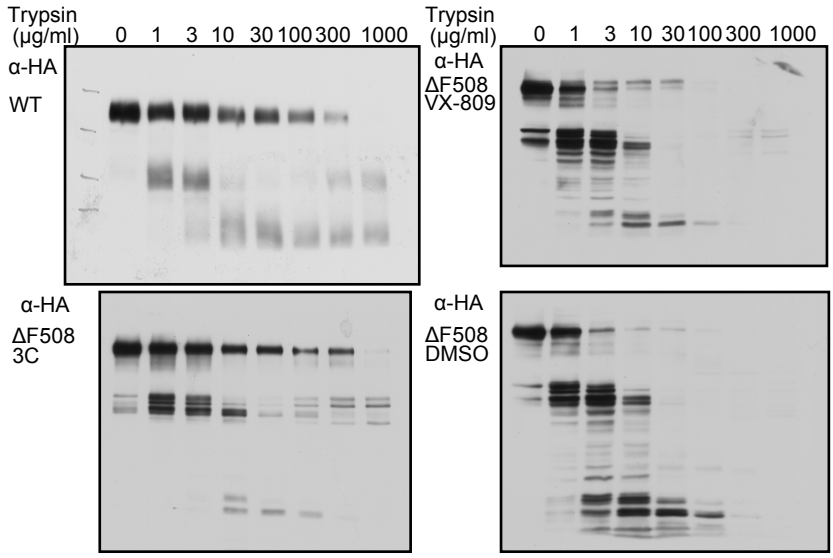

Fig. 6b

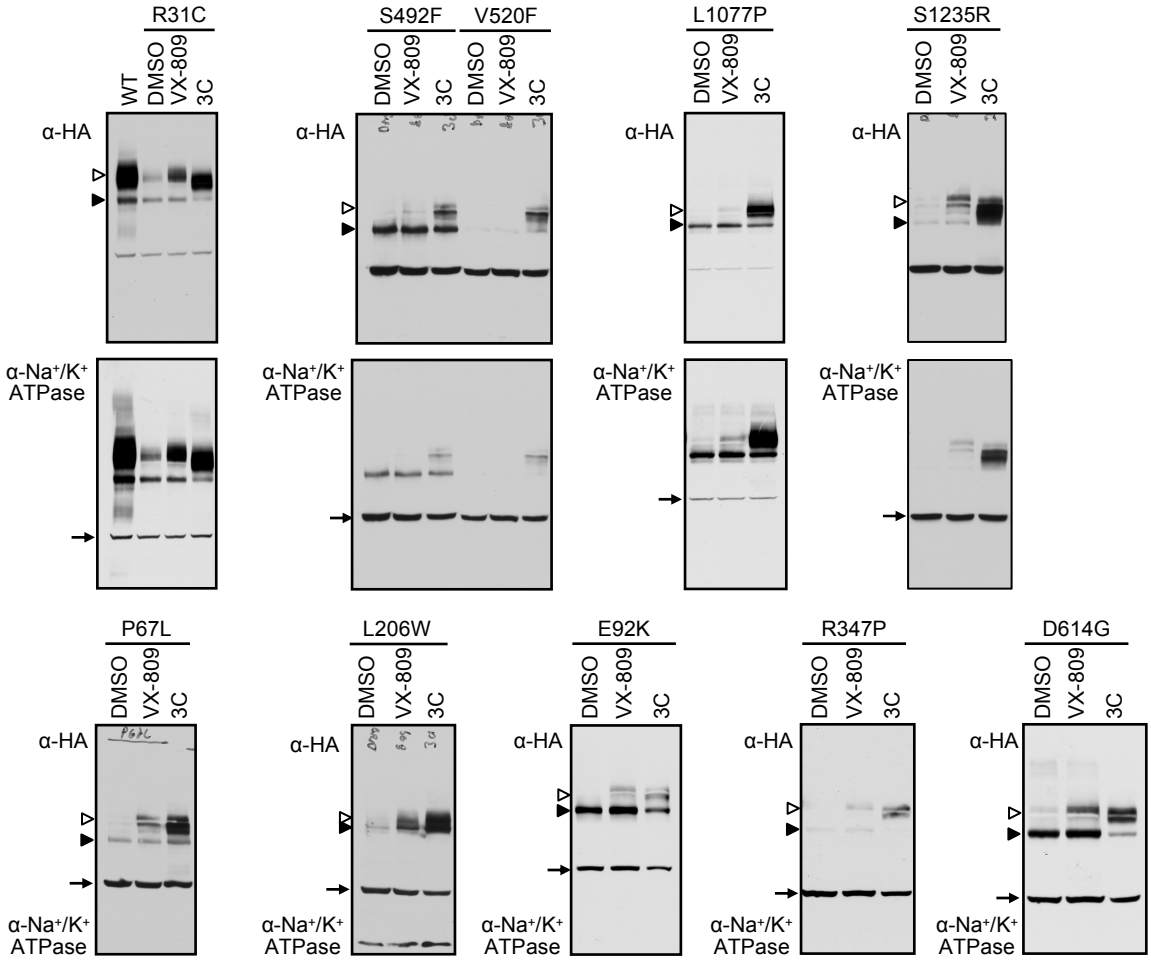

Supplementary Figure 11 - continued. Full size views of autoradiographs and western blot films displayed in cropped formats in Figures 2e, 3b, 3e, 3f, 4a and 6b. Where applicable, the core- and complex-glycosylated form of CFTR are indicated by filled and empty arrowheads, respectively, and the loading control by arrow.

Supplemental tables

Supplementary Table 1. Corrector potency in ΔF508-CFTR CFBE41o- measured with or without VX-809. Dose-response fitting was performed with the mean data shown in **Fig. 1d-f** and **Supplementary Fig. 1d-e.**

Compound	EC_{50} PM density (μM)	EC_{50} function (μM)	EC_{50} PM density (μM) + 3 μM VX-809	EC_{50} function (μM) + 3 μM VX-809
6258	0.26	0.16	n.d.	n.d
3170	2.34	1.21	n.d.	n.d
6224	0.71	0.34	n.d.	n.d
3151	n.d.	n.d.	4.82	4.20
3140	n.d.	n.d.	1.25	3.27
3152	n.d.	n.d.	1.26	2.96
3154	n.d.	n.d.	2.17	0.36
3149	n.d.	n.d.	0.82	1.96
3150	n.d.	n.d.	0.82	2.04
4172	2.53	3.11	n.d.	n.d.
3158	4.14	3.97	n.d.	n.d.
3159	4.88	8.04	n.d.	n.d.
2216	6.01	4.12	n.d.	n.d.
3835	4.00	5.93	n.d.	n.d.
3836	10.57	3.95	n.d.	n.d.

n.d.- not determined

Supplementary Table 2. Corrector affinity for binding to CFTR-NBD1 variants.

Compound	ΔF508-NBD1-1S Mean K_D ± SEM (μM)	ΔF508-NBD1-3S Mean K_D ± SEM (μM)	WT-NBD1-1S Mean K_D ± SEM (μM)
4172	38 ± 12 (n = 4)	48 ± 7 (n = 5)	40 ± 13 (n = 3)
BIA	2235 ± 685 (n =4)	1508 ± 587 (n = 5)	964 ± 321 (n = 4)
6258	n.b. (n = 2)	n.b.(n = 2)	n.b. (n = 4)
3151	n.b. (n = 2)	n.b. (n = 2)	n.b. (n = 4)

n.b. - no binding

Supplementary Table 3. Basal and corrected I_{sc} in CF-HNE from individuals homozygous for ΔF508. Mean ± SEM (*n* = 3).

Patient code	Age/gender	ΔI_{sc} $CFTR_{inh}$-172 DMSO (μA/cm^2)	ΔI_{sc} $CFTR_{inh}$-172 VX-809 (μA/cm^2)	ΔI_{sc} $CFTR_{inh}$-172 3C (μA/cm^2)
HNE037	53/f	2.03 ± 0.09	6.06 ± 0.38	12.23 ± 0.93
HNE049	44/m	1.36 ± 0.18	4.93 ± 0.38	7.54 ± 0.73
HNE134	35/f	1.52 ± 0.05	4.42 ± 0.13	8.50 ± 1.58
HNE152	35/m	1.23 ± 0.01	2.70 ± 0.07	3.36 ± 0.20
HNE197	31/m	1.11 ± 0.11	3.12 ± 0.48	9.99 ± 1.29
HNE211	30/f	1.30 ± 0.11	3.28 ± 0.29	6.03 ± 0.57
HNE240	28/m	0.94 ± 0.37	4.24 ± 0.59	4.62 ± 0.25
HNE263	29/f	0.82 ± 0.13	2.87 ± 0.18	5.01 ± 0.22
HNE278	25/f	4.44 ± 0.23	8.45 ± 0.35	11.36 ± 0.06
HNE302	22/f	0.95 ± 0.08	2.65 ± 0.23	6.24 ± 0.22
HNE304	23/m	0.86 ± 0.21	4.04 ± 0.38	8.32 ± 0.35
HNE318	23/f	1.22 ± 0.15	2.39 ± 0.25	3.22 ± 0.16
HNE353	22/m	1.28 ± 0.12	2.28 ± 0.40	6.63 ± 3.30
HNE373	40/f	1.57 ± 0.07	7.66 ± 1.47	13.38 ± 1.89
HNE383	21/m	1.83 ± 0.59	4.08 ± 0.30	6.35 ± 0.57
HNE418	20/m	1.37 ± 0.06	3.35 ± 0.12	3.48 ± 0.12
HNE455	29/f	3.42 ± 0.73	8.41 ± 1.32	11.03 ± 2.09